A ROBUST ABSOLUTE DETECTION EFFICIENCY CALIBRATION METHOD UTILIZING BETA/GAMMA COINCIDENCE SIGNATURES AND ISOTOPICALLY PURIFIED NEUTRON ACTIVATED RADIOXENON ISOTOPES

Justin I McIntyre, Matthew Cooper, James Ely, Derek Haas, and Brian T. Schrom

Pacific Northwest National Laboratory

Sponsored by the National Nuclear Security Administration
Award No. DE-AC05-RLO1830/PL10-ASAR-NDD05

ABSTRACT

Efforts to calibrate the absolute efficiency of gas cell radiations detectors have utilized a number of methodologies which allow adequate calibration but are time consuming and prone to a host of difficult-to-determine uncertainties. A method that extrapolates the total source strength from the measured beta and gamma gated beta coincidence signal was developed in the 1960's and 1970's. It has become clear that it is possible to achieve more consistent results across a range of isotopes and a range of activities using this method. Even more compelling is the ease with which this process can be used on routine samples to determine the total activity present in the detector. Additionally, recent advances in the generation of isotopically pure radioxenon samples of Xe-131m, Xe-133, and Xe-135 have allowed these measurement techniques to achieve much better results than would have been possible before when using mixed isotopic radioxenon source. This paper will discuss the beta/gamma absolute detection efficiency technique that utilizes several of the beta-gamma decay signatures to more precisely determine the beta and gamma efficiencies. It will than compare these results with other methods using pure sources of Xe-133, Xe-131m, and Xe-135 and a Xe-133/Xe-133m mix.

OBJECTIVES

Efforts to calibrate radiation detectors remains one of the most challenging tasks for manufacturers and operators and is frequently the most significant source of systematic error reported in activity concentration measurements. Calibration methods typically rely on using carefully produced calibration standards and in-depth geometry modeling, both of which are time consuming and, in the case of modeling, uses idealized versions of detectors that may differ significantly from the actual detector being calibrated [Keillor 2009]. Other methods to measure the absolute activity use beta-gamma coincidence counting or differential length proportional tubes [NCRP 1985] to leverage 2 or more parameters to determine the detection efficiency. These techniques frequently are employed to determine the activity of standards which are later used to calibrate other detectors. An ideal solution is to use a source of moderately well-known activity (~±10%) to precisely determine the detector efficiencies, energy range and resolution. While such a generalized technique is applicable across all geometries of detectors and all types of radioactive decays, the extrapolation method for radioxenon discussed in this paper utilizes detectors that subtend very high solid angles, use radioactive isotopes that decay via beta-gamma coincidences and builds upon past efforts in the CTBTO radioxenon community [Axelsson 2003, Cooper 2011, Haas 2009, McIntyre 2009]. These two elements ensure the spectral extrapolation technique is accurate and easily implemented.

The beta-gamma coincident detectors used at the Pacific Northwest National Laboratory are used to detect very low levels of radio-xenon activities that may be associated with underground nuclear tests [CTBTO 1999, Auer 2004, Ringbom 2003, Fontaine 2004]. The four radio-xenon isotopes are ^{133}Xe, ^{133m}Xe, ^{131m}Xe, and ^{135}Xe and Table 1 shows the dominate decays for the two isotopes investigated here; ^{133}Xe and ^{135}Xe. Additionally, ^{222}Rn and its daughter products, ^{214}Pb and ^{214}Bi, are used to calibrate the gamma and beta energy scales. Radon-222 is also used to determine the interference ratios because its daughter products can be an undesirable contaminate in the purified xenon gas samples. Several scheme and hardware modifications have been developed to calibrate the detectors or make the setup and calibration of the detectors easier [Reeder 2004, Cooper 2007]. The early beta-gamma spectrometer used several photo-multiplier tubes (PMT's) that had to be gain matched for both the gamma/x-ray spectrometer and for the beta/CE beta cells [Reeder 1998]. This hardware setup prevented the detectors from being simultaneously calibrated, and caused cross contamination of samples due to the close proximity of the beta detectors and the 4-well NaI(Tl) saddle detector.

The improved beta-gamma detectors used independent gamma/x-ray detectors and single PMT beta cells to significantly reduce the detector setup complexity and allow for independent simultaneous calibration of the four detectors [Cooper, 2005]. With the development of pure radioxenon samples (^{133}Xe, ^{135}Xe and ^{131m}Xe) via neutron activation much of the difficulty associated with overlapping beta and gamma signatures from multiple isotopes was minimized or eliminated [Haas DA 2009]. The interference of the ^{135}Xe isotope was the last of the interference terms to be measured and quantified, and its contribution to the measurement of the ^{133}Xe and ^{133m}Xe concentration has been properly accounted for and reduced [Ely 2011]. The pure radioxenon spikes also allow the use of spectral extrapolation techniques to more accurate determine the beta-gamma efficiency for each of the dominate decays for three of the four radioxenon isotopes

Research Accomplished

An initial investigation of using spectral extrapolation to determine the beta and gamma efficiency for ^{133}Xe and ^{135}Xe was done and has been outlined in a recent paper [McIntyre 2012]. Recently, more advanced methods have since been employed that provide more consistent results. Figure 1 show the beta distribution from calibration spectra of ^{131m}Xe, ^{133}Xe and ^{135}Xe and figure 2 shows the gamma distributions for the same isotopes. Note that the log scale clearly shows additional gamma peaks that are not used in the analysis nor in the determination of the concentrations as they are normally too small to be seen. The ^{131m}Xe beta distribution shows the conversion electron peak that is in coincidence with the ~30-keV x-rays. The ^{135}Xe beta distribution on the hand is a pure beta

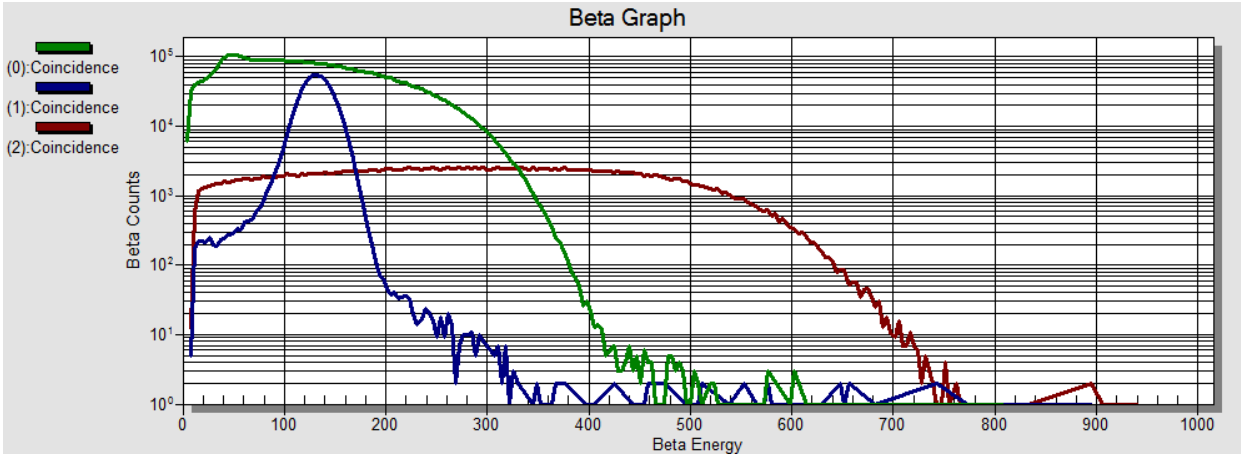

Figure 1. Histogram of the beta energy distributions for three of the four isotopes measued, ^{133}Xe is green, ^{135}Xe is brown and ^{131m}Xe is blue.

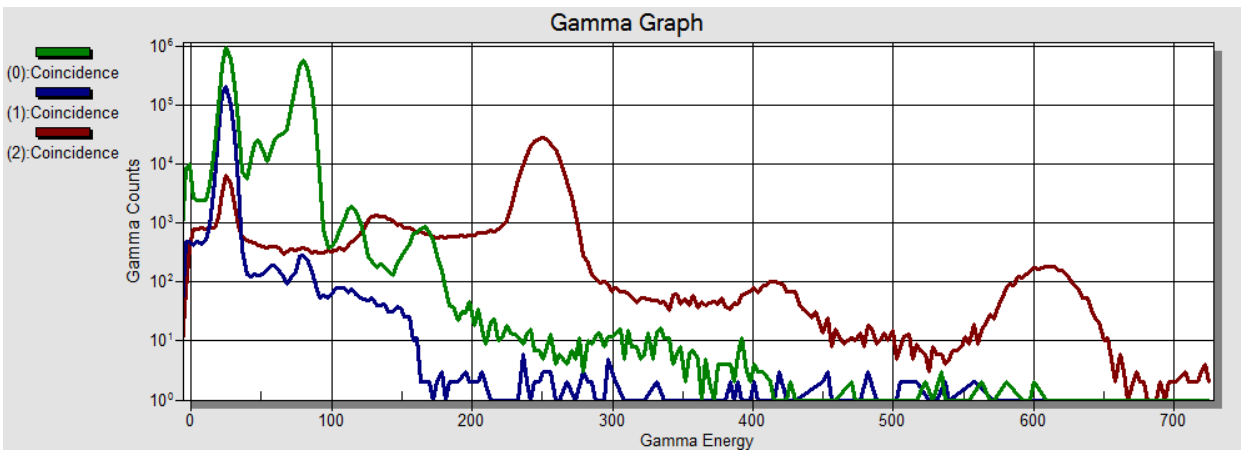

Figure 2. Histogram of the gamma energy distributions for three of the four isotopes measued, ^{133}Xe is green, ^{135}Xe is brown and ^{131m}Xe is blue. Not all of the peaks are used for quantification of the xenon concentrations.

distribution that starts at 0-keV and extends to the beta end point (910 – keV) or the maximum beta energy deposited in the 2.0 mm beta cell (~ 750-keV as seen).

Current Calibration Approach

The current approach to calibration of the beta-gamma detectors is using high activity samples of individual isotopes to determine the efficiency of the beta and gamma detectors for the regions of interest for each isotope. The primary region of interest for ^{135}Xe is the 250 keV gamma ray peak. For the ^{133}Xe, the primary regions of interest are the 80 keV gamma peak and ~ 30 keV areas for the x-rays. The beta regions of interest extend from the lowest measureable response to the beta endpoint energies. The background subtracted counts *N* for each region are related to the total activity *A* by the efficiency *ε* for each detector, and the branching ratio (*BR)* into the specific region of interest:

$$A = \frac{N_\beta}{\varepsilon_\beta BR_\beta} = \frac{N_\gamma}{\varepsilon_\gamma BR_\gamma} = \frac{N_{\beta\gamma}}{\varepsilon_{\beta\gamma} BR_{\beta\gamma}} \qquad \text{Eq. 1}$$

where the subscripts designate the beta, gamma, and beta-gamma coincidences. With the assumptions that each detector only detects specific radioactivity (i.e. electrons or photons only) and that the beta-gamma efficiency or

branching ratio is simply the product of the individual beta and gamma efficiency or branching ratio, the above equations can be rearranged to provide the beta and gamma detector efficiency for the specific region of interest:

$$\varepsilon_\beta = \frac{N_{\beta\gamma}}{N_\gamma BR_\beta}; \quad \varepsilon_\gamma = \frac{N_{\beta\gamma}}{N_\beta BR_\gamma};$$

Eq. 2a,b

This method provides a fairly simple methodology to determine the efficiencies without requiring prior knowledge of the activity of the sample, which is challenging to do because the radioxenons samples are a gas and they are short lived. The efficiencies derived in this fashion have some uncertainty associated with them due to the fact that the beta detector is not 100% efficient and, in addition to betas, they also detect conversion electrons and low energy x-rays.

<u>1-Dimensional Extrapolation Approach</u>

Following the formalism developed by Baerg 1973 and others the more general form of the relationship between the net counts and activity becomes more complicated. For example, the relationship between the counts in the beta detector (all counts) is related to the total activity by:

$$N_\beta = A\sum BR_r\left[\varepsilon_{\beta r} + \left(1-\varepsilon_{\beta r}\right)\left(\frac{\alpha\varepsilon_{CE}+\varepsilon_{\beta\gamma}}{1+\alpha}\right)_r\right]$$

Eq. 3

Where the BR_r is the beta branching ratio for the rth branch, α is the total internal conversion coefficient, and the efficiencies are for the betas (β), conversion electrons (*CE*) and for the beta detector to detect gammas (βγ). There are similar complicated expressions for the gamma and coincidence count relationships to the total activity, and it becomes challenging to determine the effective efficiency, especially since there are multiple efficiencies for each of the detector types.

To provide a more precise detector calibration for the radioxenons a different approach was investigated. This approach is to use the one dimensional extrapolation method developed several decades ago for absolute activity measurements with beta-gamma detectors. This approach assumes the counts are all related by a function *F* that can be extrapolated to obtain the total activity:

$$N_\beta = F\left(N_{\beta\gamma}/N_\gamma\right), \quad N_\beta \to \left[F(1)=A\right] \quad as \quad N_{\beta\gamma}/N_\gamma \to 1$$

Eq. 4

The benefit of this approach is that the various efficiencies, coefficients or branching ratios do not need to be known beforehand. The total activity can be calculated by fitting the distribution of counts from the beta detector as a function of the ratio of coincidence to gamma counts, typically with a low order polynomial, and then extrapolating the result to 1. The distribution is generated by changing the beta detector efficiency, and for this investigation, the data was collected with multichannel analyzers and the lower energy cutoff in the beta detector varied to change the beta efficiency. The changes to the lower energy cut off was done by analysis rather than changing the physical lower level discriminator of the multi-channel analyzer. With the known activity from the extrapolation, the effective efficiency for beta-gamma coincidences determined for each specific region of interest can then be determined for an accurate calibration of the detector system. Figure 3 shows the gamma singles spectrum (blue curve), along with the beta-gated gamma spectrum (red curve) and additional beta-gated gamma spectra with increasing software cuts on the beta distribution data for a ^{133}Xe sample (green, purple and light blue curves). This is shown in figure 3 as the green, purple and light blue curves where an increasing number of the beta channels are excluded in the sum of the beta-gated gamma's.

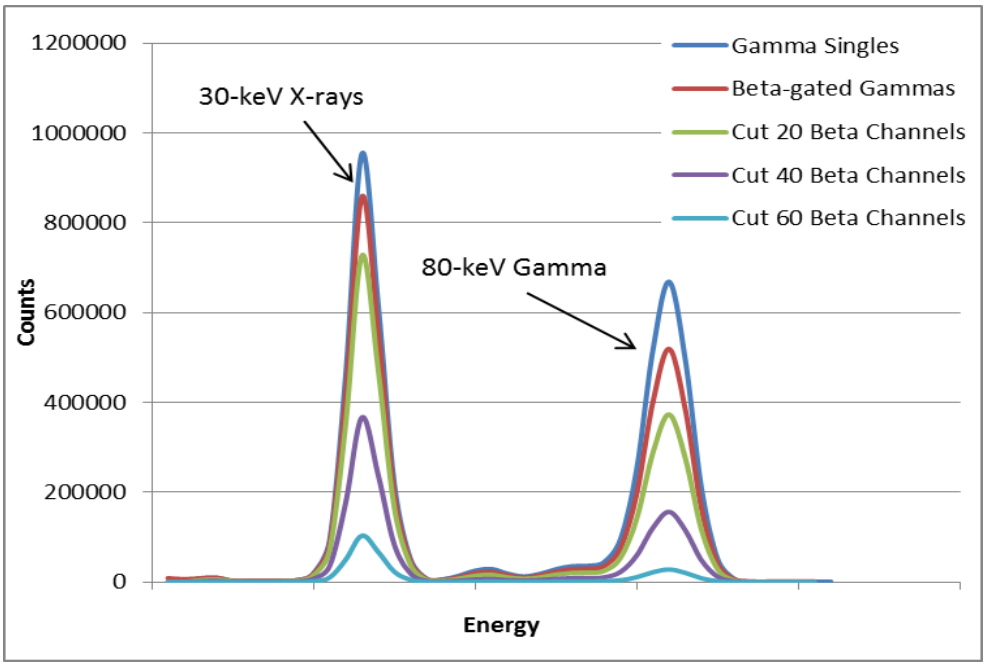

Figure 3. Histogram showing the different beta-gated gamma curves for differing beta detection efficiency (see text for further details).

Figure 4 shows the results for the one-dimensional analysis extrapolation for a modeled Xe-133 sample, where the y-axis is the number of beta singles, N_β, and the x-axis is the term 1- $N_{\beta\gamma}$ / N_γ. The y-intercept on the graph (or when the beta efficiency is 100%) for each of the distributions then becomes the total activity. As can be seen from the graph the 30 and 80-keV distributions are nonlinear and only the sum is linear which provides a very accurate

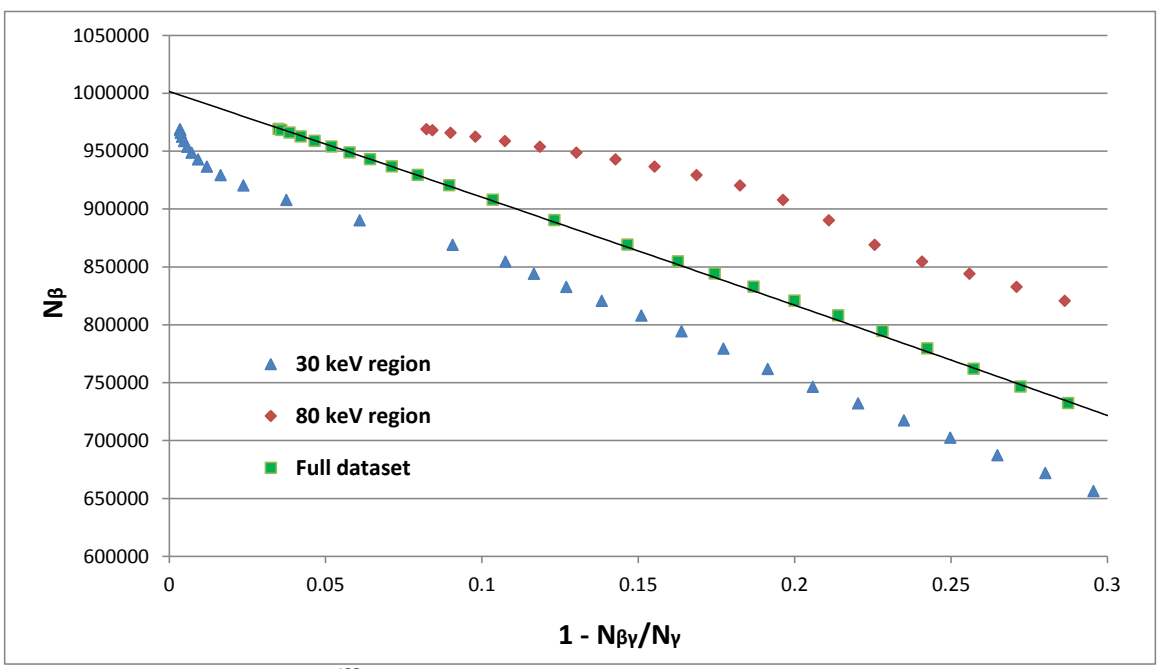

Figure 4. Modeled distribution of ^{133}Xe 30, 80 and sum coincident beta distributions vs. beta singles. The sum distribution has been fit with a a 2nd order polynomial extrapolation line to show the extrapolation of *A* when the beta efficiency is 100%.

estimate of the total activity of ^{133}Xe in the sample which was chosen to be 1,000,000 decays. The nonlinear elements in 30-keV and the 80-keV only curves arise from the difference between the 30 and 80-keV beta distributions $N_{\beta\gamma 30,80}$ and the total beta distribution N_{β} which is the combination of at least three different beta/CE distributions. For example an 80-keV *CE* in coincidence with the beta. The green data points curve, which represents the sum of the 30 and 80-keV coincidence data sets, demonstrates that the coincidence sum is a much better representation of the beta singles distribution and as such is nearly linear. The y-axis interception point is within 0.2% of the source strength (1,000,000 data points) and thus shows the power of the 1-D extrapolation technique. Similar results for the activity were obtained for ^{135}Xe, but because the decay is dominated by the 250-keV gamma-line decay (90.0%) the coincident 250-keV results very closely matched (within 0.1%) the coincident beta sum (which included a 5% BR for a 30-keV x-ray).

2-Dimensional Extrapolation Approach

From the 1-D analysis it is clear that the nonlinear nature of the various beta + CE coincident distributions arise from the variations in the beta singles distribution from those that are found for the gamma-gated distributions. This aspect suggests that if a method where developed that could remove from the beta singles the contributions from each of the different decay processes a very liner plot could be generated as seen in figure 4 for the coincident sum data sets. The y-axis intercept than becomes an estimate of the activity that is associated with for the coincident beta distribution under investigation. This estimate (which is now an scalar activity number $A_{distibution}$) can than be added back into the coincident distribution to provide a linear and hence better estimate of the overall value of *A*. This technique was developed by Smith 1975 and has since been called the 2-Dimensional extrapolation technique. Further refinement was done by Agostinelli 2003.

For ^{133}Xe there are three dominate distributions to consider, the 30-keV coincident beta-distribution, the 80-keV coincident beta distribution, and a 80-keV CE beta distribution ($N_{\beta CE80}$). The $N_{\beta CE80}$ distibution is a coincidences measurement but there is no photon in coincidence with it so it shows up in the beta-singles distribution and not as a beta-gamma distribution like the other two decay signatures. There are other decays but these are have BR less than

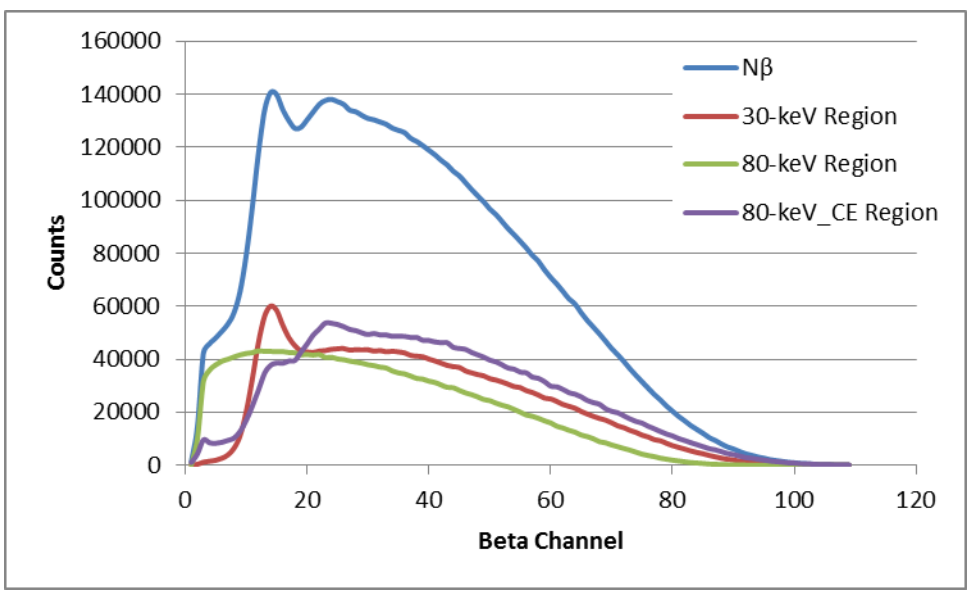

Figure 5. The raw beta distributions. Note that the beta-singles curve (N_{β}) is the sum of the other three distributions. The 30 and 80-keV curves are measured via coincidence with their repsective gamma-lines. The 80-keV CE curve is the result of subtrating the 30 and 80-keV curves from N_{β}.

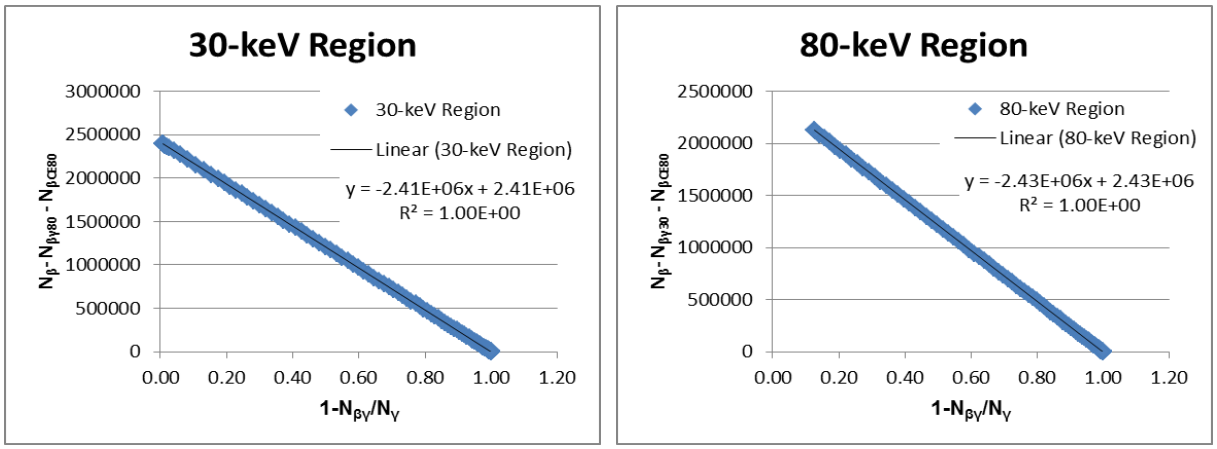

Figure 6A and B. Graphs of the 30-keV (right) and 80-keV (left) efficiencies vs. N_β minus the other beta distributions. The curves have been fit with a line and the slope and offset are identical in magnitude. The graphs show that the response is identically linear however the offsets are different as expected for a pure linear fit. The 30-keV data set (A) lies very close to the y-axis and the extrapolation to 100% efficiency (x=0) is minimal. The 80-keV data set (B) has a maximum experimentally determined efficiency .

0.2% and tend to generate L-shell x-rays (>5-keV) which are detected in the beta cell but not the NaI(Tl) well detector and so contribute to the beta singles distribution. Figure5 shows the four beta distributions and gives an indication of the difference in the overall shapes.

The beta distributions for $N_{\beta\gamma 30}$ and $N_{\beta\gamma 80}$ are estimated from the measured coincident distributions. The $N_{\beta CE80}$ distribution is estimated to be the result of subtracting $N_{\beta\gamma 30}$ and $N_{\beta\gamma 80}$ from N_β. There now three plots with different y-axis labels for figure 4. One for each of the new separate N_β distributions:

$N_\beta - N_{\beta\gamma 80} - N_{\beta CE80}$ vs. $N_{\beta\gamma 30}$; Eq. 6

$N_\beta - N_{\beta\gamma 30} - N_{\beta CE80}$ vs. $N_{\beta\gamma 80}$; Eq. 7

$N_\beta - N_{\beta\gamma 30} - N_{\beta\gamma 80}$ vs. $N_{\beta CE80}$; Eq. 8

Figure 6 shows two of graphs that are produced from these calculations and it is seen that each one can be fit with a simple linear fit. It can also be seen that both the slope of the line and the y-intercept are identical as would be expected. Essentially the 2-D extrapolation technique is plotting each of the coincident beta distributions against itself and so the result should be indentically linear. It is important to also realize that while the y-intercepts (the value of A when the beta efficiency is 100%) for each of the graphs is an estimate for the activity of that decay signature (A_{30}, A_{80}, and A_{80CE}) it will not be the absolute activity for the decay signature. It is the sum of each of the sub activities that produces the absolute activity A (ie. $A = A_{30} + A_{80} + A_{80CE}$), which can be added back into equations 6 -8.

$N_\beta - N_{\beta\gamma 80} - N_{\beta CE80} + A_{80} + A_{80CE}$ vs. $N_{\beta\gamma 30}$; Eq. 9

$N_\beta - N_{\beta\gamma 30} - N_{\beta CE80} + A_{30} + A_{80CE}$ vs. $N_{\beta\gamma 80}$; Eq. 10

$N_\beta - N_{\beta\gamma 30} - N_{\beta\gamma 80} + A_{30} + A_{80}$ vs. $N_{\beta CE80}$; Eq. 11

The offset of the linear fit for each of these graphs is than the same value and is the new best estimate of A. The slopes for each of the linear fits does not change and is still an estimate of that beta distribution's contribution to A.

The extrapolation technique lends itself easily to automated analysis as the generation of the extrapolation plots does not require analyst intervention and the fits to the data plots are simple linear plots. There are also a number cross

correlation checks that can be made to indicate whether a problem has occurred in the analysis, such as the slope and intercept for the individual beta distributions. The linearity of the fit can be checked as well by fitting the distributions with a quadratic fit, and the 2nd order parameter provides a measure of the goodness of the linear fit, large values indicate poor linear fit and small values indicate a good linear fit. For the data presented here the 2nd order parameters where of the order 10^{-7} and so were very small.

It is very important that the energy scales be accurate prior to analysis so that the energy ranges for the gamma/x-rays are appropriate and that the beta distributions cover the full range of detection. Also of importance is the large number of counts needed to achieve the high accuracy that this method can achieve (typically < 0.5%). Table 1 shows the good agreement between the detector efficiencies that were obtained with the extrapolation method vs. the current standard calibration method.

Table 1. Comparison of the detector efficiency's using the standard calibration method and the extrapolation method.

	Standard	**Extrapolation**
30-keV Gamma Efficiency	0.6514 ± 0.0124	0.6532 ± 0.0052
30-keV Region Beta Efficiency	0.9869 ± 0.0021	0.9931 ± 0.0078
80-keV Gamma Efficiency	0.7878 ± 0.0015	0.8016 ± 0.0069
80-keV Region Beta Efficiency	0.8921 ± 0.0031	0.8749 ± 0.0070
250-keV Gamma Efficiency	0.6312 ± 0.0015	0.6110 ± 0.0049
250-keV Region Beta Efficiency	0.9113 ± 0.0019	0.9060 ± 0.0073

CONCLUSIONS AND RECOMMENDATIONS

Using the extrapolation technique to determine the total source activity agrees well with other calibration methods. The technique can be automated within the Java-based calibration program currently under development at PNNL. In conclusion, the use of the extrapolation technique is both simple and robust and will allow non-experts to quickly and accurately calibrate sophisticated beta/gamma detectors. Additional work is ongoing to apply the technique to the two meta-stable isotopes ^{131m}Xe and ^{133m}Xe. However these two isotopes are well covered by the calibration using ^{133}Xe and ^{135}Xe. The use of 222Rn for a full calibration of the beta-gamma detectors has been investigated but current work indicates that the extrapolation technique is not suited to ^{222}Rn and its several daughter products.

ACKNOWLEDGEMENTS

We would like to thank the DOE for sponsorship of this work; U. S. Department of Energy, Office of Nonproliferation and National Security, Office of Research and Development.

REFERENCES

A Handbook of Radioactivity Measurements Procedures (1985). NCRP Report No. 58, 2nd edition, National Council on Radiation Protection and Measurements, Bethesda, MD, 74–93.

Agostinelli S. *et al*. (2003) Nucl. Instr. And Meth. A506:250-300

Auer M, *et al*. (2004) *Applied Radiation and Isotopes* 60(6):863-877.

Axelsson A, Ringbom A (2003) FOI-R-0913-SE.

Baerg, AP, (1973) Nucl. Instr. And Meth. 112:143-150

Cooper M, *et al.* (2011) *Proceedings of the 33rd Monitoring Research Review: Ground-Based Nuclear Explosion Monitoring Technologies*, LA-UR-11-04823:659-663

Cooper M. W *et al.* (2005). Improved β-γ coincidence detector for radioxenon detection, in *Proceedings of the 27th Seismic Research Review: Ground-Based Nuclear Explosion Monitoring Technologies*, LA-UR-05-6407, Vol. 2, pp. 779–786.

CTBTO Operational Manual for Radionuclide and the International Exchange of Radionuclide Data (1999) Preparatory Commission for Comprehensive Nuclear-Test-Ban-Treaty Organization, CTBT/WGB/TL-11/5/Rev. 4

Ely J, M. Cooper, D. Haas, J. Hayes, T. Heimbigner, and B. Schrom (2011) Monitoring Research Review, Ground-Based Nuclear Explosion Monitoring Technologies, LA-UR-11-04823:664-670

Fontaine, J. P., F. Pointurier, X. Blanchard, and T. Taffary (2004). Atmospheric xenon radioactive isotope monitoring. *J. Environ. Radioact*. 72: 129–135.

Haas DA, *et al.* (2009) *J. Radioanalytical and Nuclear Chemistry* 282 (3):677-680

Keillor ME, Cooper MW, Hayes JC, McIntyre JI (2009) *J. Radioanalytical and Nuclear Chemistry* 282(3):699-702

McIntyre JI, MW Cooper, AJ Carman, TW Bowyer, AR Day, DA Haas, JC Hayes, TR Heimbigner, CW Hubbard, KE Litke, MD Ripplinger, and R Suarez (2009). "Concentration Independent Calibration of a β-γ Coincidence Detector Using 131mXe and 133Xe". *J. Radioanal. Nucl. Chem*. 282(3):755–759.

McIntyre JI, BT Schrom, MW Cooper, DA Haas, and JC Hayes (2009). "Beowulf - Beta-Gamma Detector Calibration Graphical User Interface." Monitoring Research Reviews, Ground-Based Nuclear Explosion Monitoring Technologies, Los Alamos National Laboratory, LA-UR -09-05276: 779-787.

Reeder P.L., T.W. Bowyer, J.I McIntyre, W.K. Pitts, A. Ringbom, C. Johansson (2004) "Gain calibration of a β/γ coincidence spectrometer for automated radioxenon analysis, *Nucl. Inst. Meth Phys. Res.:A*, 521:2-3, 586–599.Cooper MW, *et al.* (2007) Nucl. Instr. And Meth. A579(1):426-430.

Reeder PL, Bowyer T W, Perkins RW (1998) Journal of Radioanalytical Nuclear Chemistry 235(1–2):89–94

Ringbom A, *et al*. (2003) Nucl. Instr. And Meth. A508:542 -553

Smith D, Stuart LEH (1975) Metrologia 11:67-72